Chinese Herbal Medicines 12 (2020) 273–280

Contents lists available at ScienceDirect

Chinese Herbal Medicines

journal homepage: www.elsevier.com/locate/chmed

Original Article

Jinbei Oral Liquid ameliorates bleomycin-induced idiopathic pulmonary fibrosis in rats via reversion of Th1/Th2 shift

Xiao-yan Xing [a,c,1], Wei-jie Qiang [a,c,1], Jia-le Bao [a], Rui-chuang Yang [d], Jun Hou [d], Kai Tao [e], Zhao-qing Meng [b], Jing-hua Zhang [b], Ai-jun Zhang [b,*], Xiao-bo Sun [a,c,*]

[a] Institute of Medicinal Plant Development, Chinese Academy of Medical Sciences and Peking Union Medical College, Beijing 100193, China
[b] Shandong Hongjitang Pharmaceutical Group Co., Ltd., Jinan 250000, China
[c] Key Laboratory of New Drug Discovery Based on Classic Chinese Medicine Prescription, Chinese Academy of Medical Sciences, Beijing 100193, China
[d] Research Center for Clinical and Translational Medicine, Fifth Medical Center, General Hospital of Chinese PLA, Beijing 100039, China
[e] The Affiliated Hospital of Shandong University of TCM, Jinan 250011, China

ARTICLE INFO

Article history:
Received 9 January 2020
Revised 17 March 2020
Accepted 27 March 2020
Available online 26 May 2020

Keywords:
bleomycin
cytokines
idiopathic pulmonary fibrosis
Jinbei Oral Liquid
Th1/Th2 shift

ABSTRACT

Objective: Idiopathic pulmonary fibrosis (IPF) is a progressive and lethal interstitial lung disease with high mortality. The pivotal role of Th1/Th2 immunological balance in the development and progression of IPF has been demonstrated previously. This study aimed to evaluate the effect of Jinbei Oral Liquid (JBOL) on IPF and its relationship with Th1/Th2 shift.

Methods: Rats were divided into six groups: control group, model group (bleomycin), pirfenidone group (positive group, 54 mg/kg, i.g.) and JBOL (5.4, 10.8 and 21.6 mL/kg, i.g.) groups. The rat model was established by an intratracheal instillation of bleomycin (BLM, 5 mg/kg). One day after injection of BLM, pirfenidone or JBOL was given to rats once daily within 28 consecutive days, respectively. Positron emission tomography/computed tomography (PET/CT) was performed on the treated rats. The extent of alveolitis and fibrosis was observed by H&E and Masson trichrome staining. The contents of TGF-β1, TNF-α, IL-4 and IFN-γ were further quantified by ELISA assay.

Results: PET/CT and histopathological evidence showed the ability of JBOL to attenuate bleomycin-induced alveolitis and fibrosis extent, and the alveolitis lesion score was markedly decreased compared with the model group. The increased expression of inflammatory cytokines TGF-β1 and TNF-α induced by bleomycin was also suppressed by JBOL. The Th1 response was limited by the reduced IFN-γ after BLM administration, and the Th2 response predominated significantly marked by the increased IL-4. JBOL could increase the level of IFN-γ and markedly increased the ratio of IFN-γ/IL-4.

Conclusion: These findings suggested that JBOL may attenuate BLM-induced idiopathic pulmonary fibrosis via reducing inflammatory cell infiltration, pro-inflammatory cytokine release and excessive collagen deposition in rats. One of the mechanisms is the reversion of Th1/Th2 shift caused by BLM.

1. Introduction

Idiopathic pulmonary fibrosis (IPF) is a progressive and devastating chronic lung disease, characterized by extreme deposition of extracellular matrix and destruction of the normal lung architecture. The development of IPF results in declining lung function and eventual respiratory failure, and the mean length of survival from the time of diagnosis is three years (Strongman, Kausar, & Maher, 2018). The pathological characteristics of IPF mainly include pulmonary interstitial inflammatory cells infiltration, fibroblasts proliferation, and collagen accumulation (Fernandez & Eickelberg, 2012). Lymphocytes and monocytes produce cytokines, which induce recruit additional inflammatory cells, promote extracellular matrix production and fibrosis (El-Chemaly et al., 2018). Immune dysregulation is a central process in the pathogenesis of IPF. The clinical manifestations of chronic interstitial lung diseases are likely associated with an initial strong immune and inflammatory response to a persistent antigen or pathogen, leading to lung injury and progressive fibrosis. Some reports about the involvement of T cells in pulmonary fibrosis, which are largely conflicting, support either a pro-fibrotic or an anti-fibrotic nature in the pulmonary fibrosis (Luzina, Todd, Iacono, & Atamas, 2008).

* Corresponding authors.
E-mail addresses: 435049799@qq.com (A.-j. Zhang), sun-xiaobo@163.com (X.-b. Sun).
[1] These authors contributed equally to this work.

https://doi.org/10.1016/j.chmed.2020.05.002
1674-6384/

T cells, particularly CD^{4+} T cells, can be differentiated into at least two functional subsets during the immune response, Th1 cells and Th2 cells. Th2-mediated adaptive immune response contributes to and sustains non-resolving inflammation in the injured tissue that leads to the development of pulmonary fibrosis (Wynn, 2004). Previous studies have shown that Th1/Th2 cell immune response plays a pivotal role in the development of IPF, as these mediators can influence fibroblast activation, proliferation and collagen deposition (Sumida et al., 2008). For instance, interferon (IFN)-γ, one of the major Th1 cytokines, appears to suppress fibroblast proliferation and collagen production, while the type 2 cytokine interleukin (IL)-4 has been identified with potent stimuli for the production of fibroblast-derived extracellular matrix (Euler et al., 2019; Gharaee-Kermani, Nozaki, Hatano, & Phan, 2003; Huaux, Liu, McGarry, Ullenbruch, & Phan, 2003; Li, Liang, Huang, Wu, & Zhong, 2018). As reported, Th1/Th2 immunological balance is altered in pulmonary fibrosis patients, resulting in a Th2-dominant shift (high expression of IL-4) (Mojiri-Forushani, Hemmati, Khodadadi, & Rashno, 2018; Tang, Lei, Pan, Zhao, & Wen, 2018). IL-4 has been reported to induce collagen synthesis by culturing fibroblasts and regulating their function, and is demonstrated to be important in the switch of naive cells to the Th2 phenotype (Aoudjehane et al., 2008; Yoshimoto, 2018). The relative paucity of IFN-γ contributes to the excessive fibroblast activation, deposition of collagen and scar formation that occurs in chronic inflammatory diseases. Thus, IL-4 and IFN-γ are important regulatory factors for pulmonary fibroblasts. The Th1/Th2 paradigm, which can be evaluated by representing cytokines for IFN-γ by Th1 and IL-4 by Th2, could be considered as a new strategy of the treatment of IPF.

Jinbei Oral Liquid (JBOL), as a traditional Chinese preparation consisting of *Astragali Radix*, *Codonopsis Radix*, *Glehniae Radix*, *Salviae Miltiorrhizae Radix* et *Rhizoma*, *Angelicae Sinensis Radix*, *Chuanxiong Rhizoma*, *Lonicerae Japonicae Flos*, *Forsythiae Fructus*, *Scutellariae Radix*, *Fritillariae Cirrhosae Bulbus*, *Pinelliae Rhizoma Praeparatum Cum Alumine*, *Glycyrrhizae Radix* et *Rhizoma*, is a clinical empirical prescription of the national old Chinese medicine experts Kai Tao in treating interstitial lung disease (ILD), that is jointly developed with Shandong Hongjitang Pharmaceutical Group Co., Ltd. Despite evidences indicating that JBOL has the potential to modify oxidative stress and inflammation in IPF, the role of JBOL on the Th1/Th2 shift evoked by chronic lung fibrosis is still unclear (Zhang et al., 2018). Hence, in this study, the protective effect of JBOL on bleomycin-induced idiopathic pulmonary fibrosis in rats was investigated and the relevant mechanism in terms of the predominant cytokine profile was explored.

2. Materials and methods

2.1. Experimental animals

Male Sprague-Dawley rats (180 to 220 g, 6–8 weeks) were purchased from Vital River Laboratory Animal Technology Co., Ltd. (Beijing, China) and used after a week of acclimatization. All the animals were fed with a standard rat chow and water freely and kept in a temperature-controlled environment (20–22 °C) with an alternating cycle of 12 h light/dark. All animal experiments were carried out ethically approved by Laboratory Animal Ethics Committee in the Institute of Materia Medica, Peking Union Medical College.

All animal experiments were carried out ethically approved by Laboratory Animal Ethics Committee in the Institute of Materia Medica, Peking Union Medical College.

2.2. Drugs and reagents

Jinbei Oral Liquid (JBOL), Shandong Hongjitang Pharmaceutical Group Co., Ltd., batch number: 1708001; Bleomycin hydrochloride (BLM), Zhejiang Hisun & Pfizer Pharmaceutical Co., Ltd., batch number: Y50512; Pirfenidone, Beijing Kangdini Pharmaceutical Co., Ltd., batch number: 170402. Enzyme-linked immunosorbent assay (ELISA) kits for transforming growth factor-β1 (TGF-β1), tumor necrosis factor-α (TNF-α), interleukin-4 (IL-4) and interferon-γ (IFN-γ) were obtained from Shanghai Fusheng Industrial Co., Ltd. (Shanghai, China).

2.3. Chromatography analysis

Three main active ingredients contained in JBOL were determined by HPLC analysis, including chlorogenic acid (Wang et al., 2017), baicalin (Huang et al., 2016), and salvianolic acid B (Liu et al., 2016). This examination was performed on the Waters e2695 chromatographic system, consisting of a vacuum degassing unit, a quaternary gradient elution solvent delivery system, a standard automatic sample injector, and a column thermostat. All the separation was performed on Inertsil ODS-$3C_{18}$ analytical column (4.6 mm × 250 mm, 5 μm) and maintained at 35 °C. The mobile phase was a mixture of acetonitrile-0.1% phosphoric acid aqueous solution with the flow rate of 1 mL/min. The injection volume was 10 μL and the detector was set at 254 nm. The standard solutions of three active ingredients were prepared with methanol.

2.4. Animal groups and model establishment

After one-week adaptive feeding, 60 rats were randomly divided into six groups of 10 rats for each: control group, model group, pirfenidone group (positive group, 54 mg/kg, i.g.), low-dose JBOL group (5.4 mL/kg, i.g.), medium-dose JBOL group (10.8 mL/kg, i.g.) and high-dose JBOL group (21.6 mL/kg, i.g.). Briefly, all rats were anesthetized with 10% chloral hydrate. Then, the rats were administered a single intratracheal instillation of BLM dissolved in physiological saline (5 mg/kg body weight), and control group with the same volume of physiological saline. One day after injection, different dosages of pirfenidone or JBOL were given to the rats once daily within 28 consecutive days, while equal volume physiological saline was given to the rats in the control and model groups. All rats were weighed once a week. At day 28 after administration, all rats were used for PET/CT imaging. After PET/CT scans, these rats were sacrificed under deep anesthesia, and lung tissues were collected. The left lung was fixed in 4% paraformaldehyde for histology analysis, and the right lung was excised and washed in the ice-cold saline, then they were both quickly frozen in liquid nitrogen for biochemical studies.

2.5. Lung index detection

The frozen lungs were removed, rinsed with ice-cold physiological saline, and weighed. Lung index was calculated according to the following equation: lung index = (lung weight/body weight) × 100%.

2.6. PET/CT imaging

Positron emission tomography/CT imaging experiments were performed in rats using the Inveon small-animal PET/CT scanner (Siemens, Knoxville, TN) at day 28 after administration (three rats per group). Anesthetized rats were placed in the supine position in the PET/CT scanner and the lungs centered in the field of view. Imaging acquisition started with a low-dose CT scan and followed by a 10-minute PET scan immediately. The CT scan was used for localization of the lesion site and attenuation correction.

The reconstructed images were examined with a 3D display, in transverse, coronal and sagittal views. For each PET image, the regions of interest (ROIs) were drawn over the lesion site of lung

on each PET/CT image by using Inveon Research Workplace software.

2.7. Histopathological studies

After 3-day fixation, lung tissues were dehydrated and imbedded in paraffin. The paraffin-embedded tissue samples were sectioned into 6-μm slices and stained separately with haematoxylin and eosin (H&E) and masson trichrome (MT). Alveolitis scores were noted in H&E stained sections via semi-quantitative histology, while fibrosis scores were graded from MT stained sections (Li et al., 2017). Ten fields per section were randomly selected for per rat, and a blinded pathologist examined 10 fields per rat using an Olympus microscope (Olympus, Tokyo, Japan). The total score of each section was calculated, and the mean score of each group was determined.

2.8. Biochemical analysis

The frozen lung lobes of each animal were thawed and homogenized in the isotonic saline. The homogenates were centrifuged at 3000 rpm for 5 min, and the supernatant was collected. The levels of TGF-β1, TNF-α, IL-4 and IFN-γ in the homogenates were detected by ELISA kits in accordance with the manufacturer's instructions. The absorbance was measured using a microplate reader (Labsystems Multiskan MS) and concentrations of TGF-β1, TNF-α, IL-4 and IFN-γ were calculated by comparison curve established in the same measurement.

2.9. Statistical analysis

Data were collected and expressed as mean ± standard deviation (SD). The differences between every group were compared with one-way analysis of variance (ANOVA) followed by LSD's test. $P < 0.05$ was considered as statistically significant. Semi-quantitative data of histopathological examination were analyzed by Kruskal-Wallis test. Statistical analyses were performed using SPSS 24.0 software.

3. Results

3.1. Chromatogram of active ingredients in JBOL

As shown in Fig. 1, the S1 curve shows the fingerprint of reference mixture solution, while the S2 curve represents the fingerprint of the JBOL. Furthermore, the peak 4 is chlorogenic acid, the peak 14 is baicalin, and the peak 15 is salvianolic acid B. The contents of chlorogenic acid, baicalin and salvianolic acid B were 4.16 mg/10 mL, 2.57 mg/10 mL and 3.88 mg/10 mL, respectively. The results were in accordance with the relevant provisions of the 2015 *Chinese Pharmacopoeia* and JBOL quality standards.

3.2. Effect on body weight and lung index

There was no significant difference in the initial weight of rats in each group. Compared with the rats in the control group, treatment with BLM resulted in a marked decrease in their body weight on days 7, 14 and 28. Administration of pirfenidone or JBOL had no significant increase in their body weight compared with the model group (Fig. 2). On the other hand, lung index may reflect the degree of BLM-induced lung injury. BLM exposure resulted in a significant increase in lung index compared to the control group ($P < 0.001$), which could be significantly attenuated by JBOL medium dose (10.8 mL/kg, $P < 0.05$). However, no significant difference was observed in lung index in the pirfenidone or JBOL groups (5.4 mL/kg and 21.6 mL/kg, Fig. 3).

3.3. PET/CT imaging examination

In the control group, PET/CT scans of lung tissues exhibited a uniformly distributed lung markings and a regular interface. The alveolar septal thickness, along with the lung septal and lobular structures was normal. Differently-sized granular high-density shadows or reticular fibrous shadows were found diffusely distributed in the lungs of the rats in the model group whatever in transverse or coronal sections. Lungs in pirfenidone or JBOL groups showed scattered distribution granular high-density shadow and small pieces of reticular fibrous shadow, but the size of the parti-

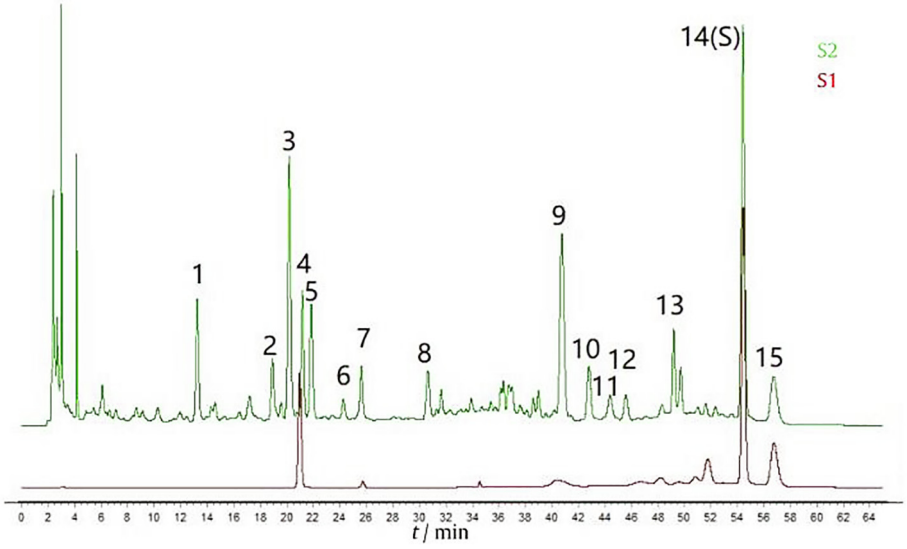

Fig. 1. HPLC chromatogram of three ingredients in JBOL. This chromatogram was performed on Inertsil ODS-3C_{18} analytical column (4.6 mm × 250 mm, 5 μm) with a mixture of acetonitrile-0.1% phosphoric acid aqueous solution as mobile phase and a flow rate of 1 mL/min. The injection volume was 10 μL and the detector was set at 254 nm. The peak 4 is chlorogenic acid, the peak 14 is baicalin, and the peak 15 is salvianolic acid B.

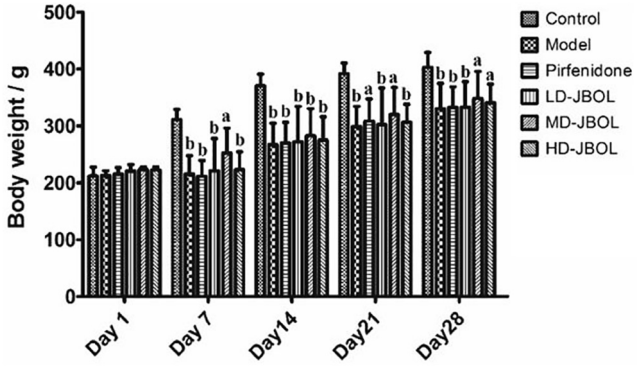

Fig. 2. Body weight in normal and BLM-induced IPF rats on days 1, 7, 14, 21 and 28 after treatment (mean ± SD, $n = 10$). $^{a}P < 0.01$ and $^{b}P < 0.001$ *vs* control group. BLM: bleomycin; IPF: idiopathic pulmonary fibrosis; LD-JBOL: low-dose JBOL group; MD-JBOL: medium-dose JBOL group; HD-JBOL: high-dose JBOL group.

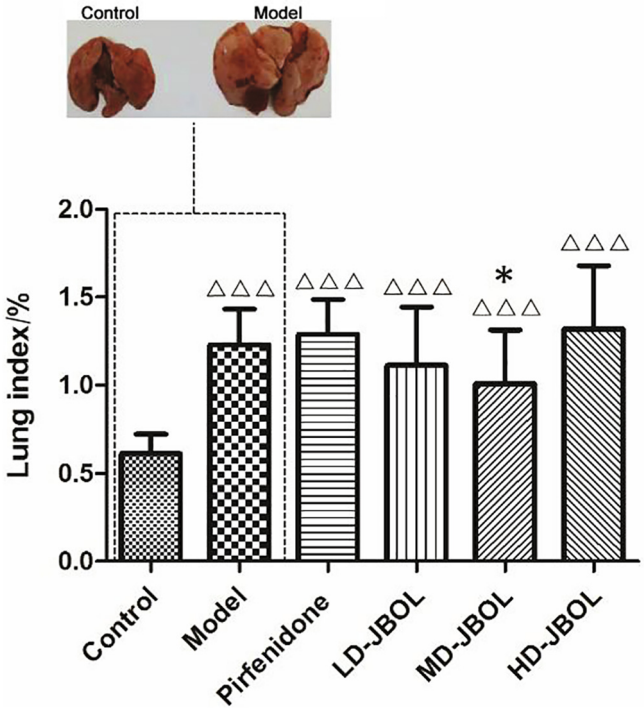

Fig. 3. Lung index of the control and BLM-induced IPF groups and the related image on day 28 after treatment (mean ± SD, $n = 10$). $^{\triangle\triangle\triangle}P < 0.001$ *vs* control group; $^{*}P < 0.05$ *vs* model group. BLM: bleomycin; IPF: idiopathic pulmonary fibrosis; LD-JBOL: low-dose JBOL group; MD-JBOL: medium-dose JBOL group; HD-JBOL: high-dose JBOL group.

cles and area of involvement were smaller than those in the model group (Fig. 4).

3.4. Effect on bleomycin-induced histopathology observation

Histopathological abnormalities in lungs were detected by H&E staining (Fig. 5) and MT staining (Fig. 6) at the end of treatment on day 28. As shown in Fig. 5A, the lung tissues in rats in the control group showed normal alveolar structure, intact pulmonary vascularity, absence of inflammation and normal alveolar septa. However, the alveolar space of the rats in the model group marked inflammatory exudation and inflammatory cells infiltration, mainly lymphocytes and neutrophils. In addition, the pachyntic

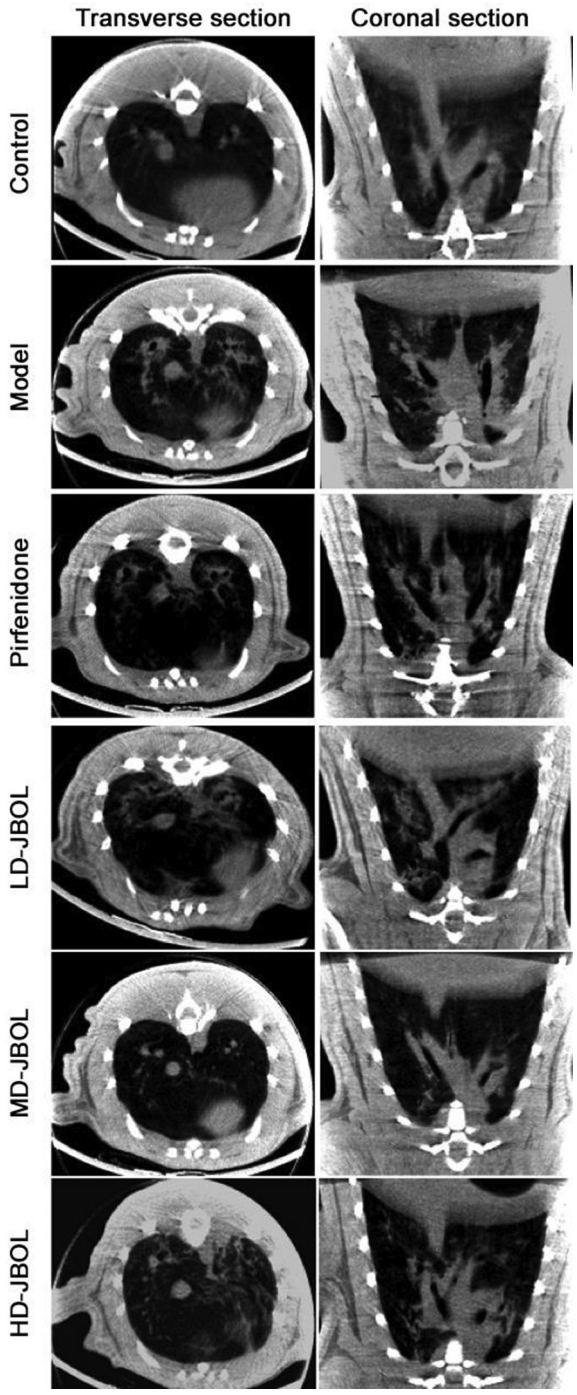

Fig. 4. Representative transverse (left) and coronal (right) sections of PET/CT images in rats with BLM-induced IPF on day 28 after treatment. BLM: bleomycin; IPF: idiopathic pulmonary fibrosis; LD-JBOL: low-dose JBOL group; MD-JBOL: medium-dose JBOL group; HD-JBOL: high-dose JBOL group. Control: The image shows that the lungs of the control group were normal in texture, and there was no obvious abnormal density, and the size of heart shadow was not abnormal. Model: The image shows that the model group of rats has a typical structural abnormality of the lung tissue, which has a honeycomb shape, a patchy consolidation in the lower lobe of the left lung, and a small patch of ground glass in the posterior segment of the right upper lobe. The base is fused into a larger range of solid shadows with blurred edges. Pirfenidone: The image shows a small number of irregular small patch-like shadows in the lower lobe of the two lungs of the pirfenidone group, with uneven density and thickened tracheal walls. The upper lobe of the right lung has a patchy ground glass shadow. LD-JBOL: The image shows irregular low-density small patchy shadows on the lower lobe of the two lungs of the low-dose group, and patchy ground glass shadows on the right upper lobe. MD-JBOL: The image shows diffuse flaky and nodular shadows in the middle and lower parts of the right lung of rats in the middle-dose group, and patchy ground glass shadows in the upper lobe of the right lung. HD-JBOL: The image shows a small number of nodular shadows and sheet-like high-density shadows on the lower lobe of the two lungs of the high-dose group, and patchy ground glass shadows on the right upper lobe.

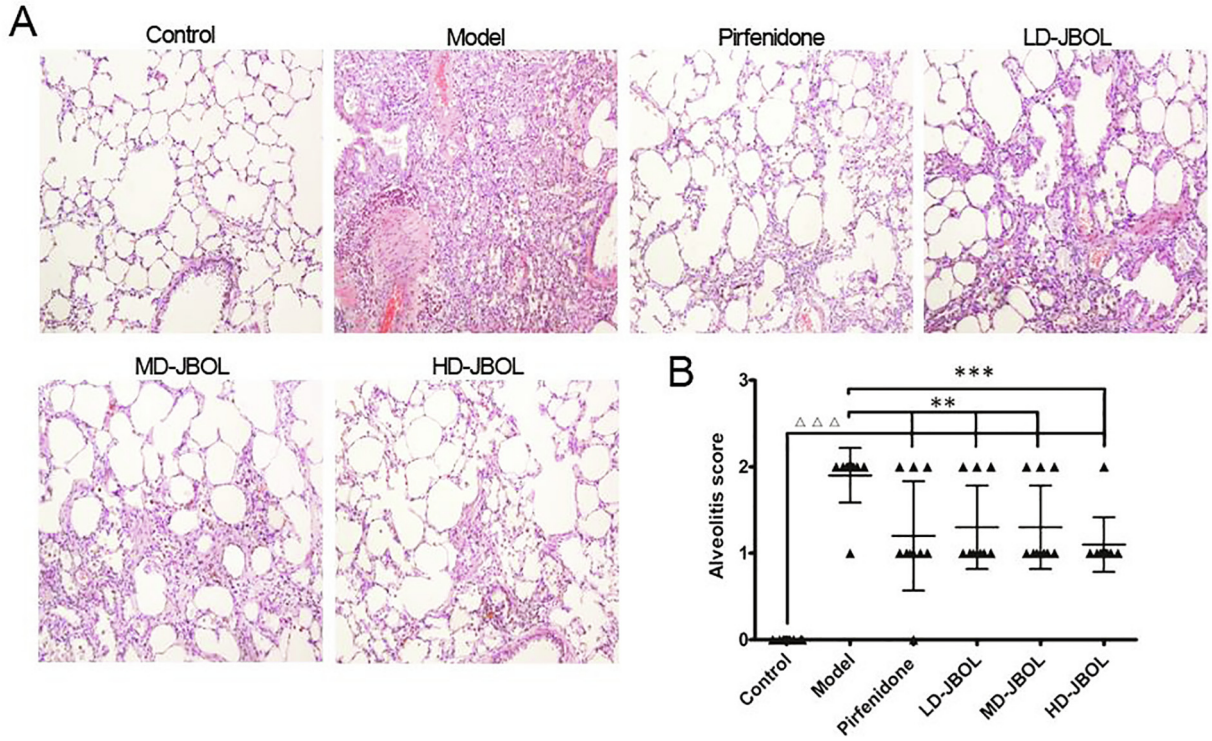

Fig. 5. Effect of JBOL on pathological changes of lung tissues in rats with BLM-induced IPF by H&E staining (magnification, ×100). (A) Representative images of H&E staining of each group on day 28 after treatment. (B) Alveolitis score was evaluated with H&E staining sections and was graded using the following criteria: none (scored 0), no alveolitis; mild (scored 1), pleural-based lesions occupying <20% of the lung and with good preservation of the alveolar architecture; moderate (scored 2), a more widespread alveolitis involving 20%–50% of the lung, although still predominantly pleural based; severe (scored 3), a diffuse alveolitis involving more than 50% of the lung, with occasional consolidation of air spaces by the intra-alveolar mononuclear cells and some hemorrhagic areas within the interstitium and/or alveolus. The evaluation was performed in a blinded manner. Results are expressed as the mean ± standard deviation. $^{\triangle\triangle\triangle}P < 0.001$ *vs* control group; $^{**}P < 0.01$ and $^{***}P < 0.001$ *vs* model group. BLM: bleomycin; IPF: idiopathic pulmonary fibrosis; H&E: hematoxylin and eosin; LD-JBOL: low-dose JBOL group; MD-JBOL: medium-dose JBOL group; HD-JBOL: high-dose JBOL group.

pulmonary interstitium and interstitial edema were observed. Scattered alveolar damage, fusion, bullae formation and accumulation of alveolar exudates were also noted. The alveolitis in each intervention group (pirfenidone or JBOL treated groups) demonstrated histological improvement. The alveolitis scores in each group were further determined and shown in Fig. 5B. Alveolitis score in model group markedly increased in comparison with the control group ($P < 0.001$), and significantly decreased by pirfenidone or JBOL treatment compared with the model group ($P < 0.01$), obviously in the JBOL 21.6 mL/kg group ($P < 0.001$).

MT staining was used to examine the extent of collagen production in IPF. MT staining revealed that the lung sections of rats in the control group exhibited normal collagen fiber distribution and small amount of staining of aniline blue, whereas an increased amount of blue collagen was deposited in the alveolar septum, bronchi and perivascular areas in the model group (Fig. 6A). Blue collagen deposition of all intervention groups was mild compared with model group, but no statistically significant was observed in fibrosis scores (Fig. 6B).

3.5. Effects on TNF-α and TGF-β1 levels in lung

As shown in Fig. 7, the concentrations of TNF-α and TGF-β1 in the model group were significantly increased compared with the control group ($P < 0.001$). JBOL (5.4, 10.8 and 21.6 mL/kg) and pirfenidone (54 mg/kg) administration led to a significant decrease in the concentrations of TGF-β1 compared with the model group ($P < 0.001$), and reduced TNF-α levels were also observed in JBOL (10.8 mL/kg and 21.6 mL/kg) and pirfenidone (54 mg/kg) groups compared to that of the model group ($P < 0.001$).

3.6. Effects on Th1/Th2 shift

The expression of IFN-γ and IL-4, which was the most representative cytokines of Th1 and Th2, was detected by ELISA. The decreasing expression level of Th1 related to cytokine IFN-γ and an increase of level of Th2 related to cytokine IL-4 were observed in the model group compared to the control group ($P < 0.001$, Fig. 8A). Meanwhile, the ratio of IFN-γ/IL-4 significant decreased in the model group in comparison with the control group ($P < 0.001$, Fig. 8B), indicating that Th2-dominant shift was presented in BLM-induced IPF. JBOL (10.8 mL/kg and 21.6 mL/kg) significantly increased the level of IFN-γ ($P < 0.001$), and JBOL (5.4, 10.8 and 21.6 mL/kg) presented an down-regulation trend to IL-4 when compared to the model group ($P < 0.001$) as shown in Fig. 8A. Corresponding to reverse the Th1/Th2 shift, an up-regulation of IFN-γ/IL-4 was also observed in all intervention groups ($P < 0.001$, Fig. 8B).

4. Discussion

In order to ensure the quality, the major compounds in the JBOL were analyzed with HPLC. According to the physicochemical properties of the components contained in JBOL, combined with the requirements of the quantitative determination of various medicinal materials in the Chinese Pharmacopoeia, the chlorogenic acid, baicalin, salvianolic acid B were used as indicator ingredients. The results showed that the three components were well absorbed at specific wavelengths, and the quality of JBOL was stable. Additionally, to evaluate the possible protective effects of JBOL on BLM-induced idiopathic pulmonary fibrosis, concentrations of

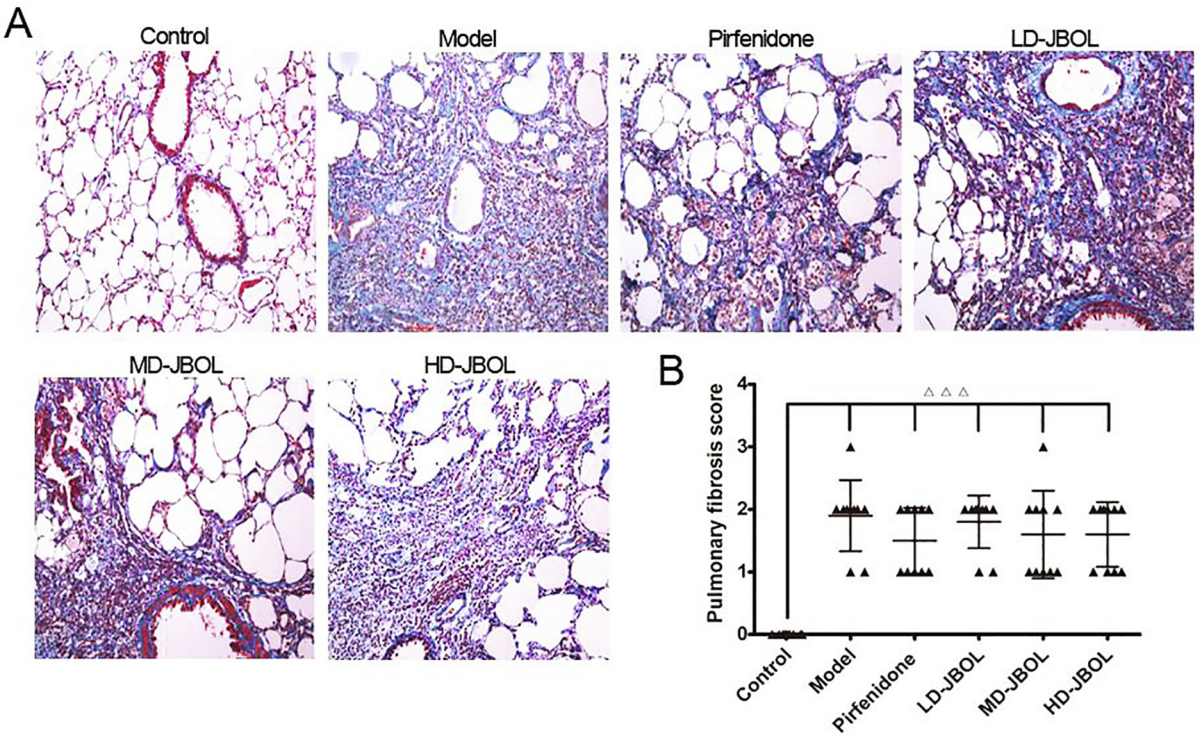

Fig. 6. Effect of JBOL on pathological changes of lung tissues in rats with BLM-induced IPF under MT staining (magnification, ×100). (A) Representative images of MT staining of each group on day 28 after treatment. (B) Pulmonary fibrosis score was evaluated with MT staining sections and was graded using the following criteria: none (scored 0), no evidence of fibrosis; mild (scored 1), focal regions of fibrosis involving <20% of the lung. Fibrosis involved the pleura and the interstitium of the subpleural parenchyma with some distortion of alveolar architecture; moderate (scored 2), more extensive fibrosis involving 20% to 50% of the lung and fibrotic regions mostly extending inward from the pleura and still focal; severe (scored 3), widespread fibrosis, involving more than 50% of the lung. Confluent lesions with extensive derangement of parenchymal architecture, including cystic air spaces lined by cuboidal epithelium. The evaluation was performed in a blinded manner. Results are expressed as the mean ± standard deviation. $^{\triangle\triangle\triangle}P < 0.001$ *vs* control group. BLM: bleomycin; IPF: idiopathic pulmonary fibrosis; MT: masson trichrome; LD-JBOL: low-dose JBOL group; MD-JBOL: medium-dose JBOL group; HD-JBOL: high-dose JBOL group.

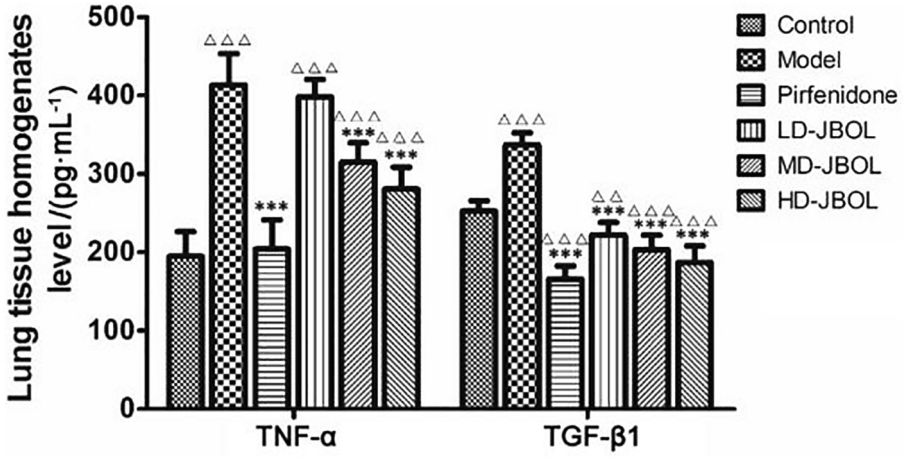

Fig. 7. Effect of JBOL on TNF-α and TGF-β1 levels in lung homogenates. Results are expressed as the mean ± standard deviation. $^{\triangle\triangle\triangle}P < 0.001$ *vs* control group; $^{***}P < 0.001$ *vs* model group. TNF-α: tumor necrosis factor-α; TGF-β1: transforming growth factor-β1; LD-JBOL: low-dose JBOL group; MD-JBOL: medium-dose JBOL group; HD-JBOL: high-dose JBOL group.

TGF-β1, TNF-α, IL-4, IFN-γ and IFN-γ/IL-4 ratio were measured in lung tissues. PET/CT imaging and histopathology observation were conducted to evaluate the interventional effects of JBOL. All the above parameters were also measured in BLM groups treated with three dosages of JBOL. The IPF model of intratracheally injecting bleomycin in rats was typically used to identify potential therapeutic interventions and to evaluate the underlying mechanisms of lung fibrosis. The pathophysiological changes and processes in the model are mostly similar to those in human pulmonary fibrosis (Peng et al., 2013; Yasui et al., 2001). The morphologies of JBOL groups showed that the states of alveolitis and collagen deposition in lungs were decreased when compared with the model group, and PET/CT revealed that the rats exhibited mild fibrosis, suggesting that JBOL had an inhibitory effect on bleomycin-induced idio-

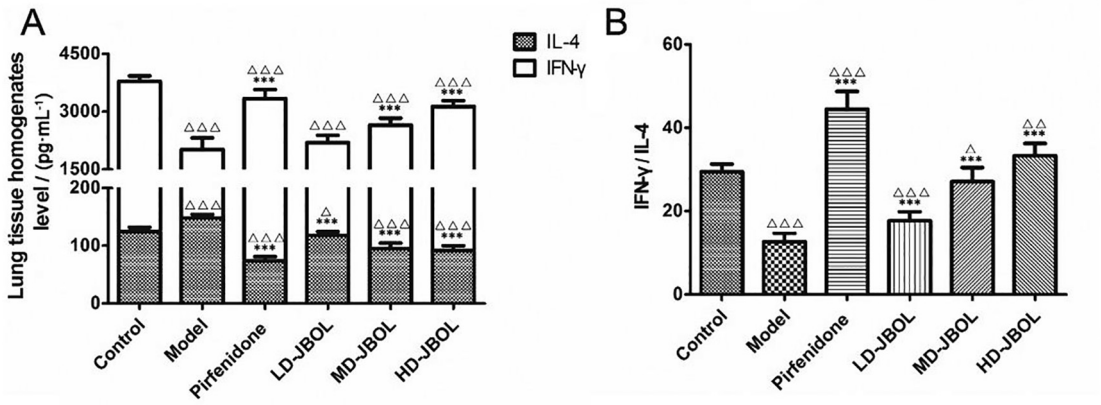

Fig. 8. Effect of JBOL on Th1/Th2 shift of lung tissues in rats with BLM-induced IPF. (A) Effect of JBOL on IL-4 and IFN-γ levels in lung homogenates. (B) Effect of JBOL on the ratio of IFN-γ/IL-4 in lung. Results are expressed as the mean ± standard deviation. $^{\triangle}P < 0.05$, $^{\triangle\triangle}P < 0.01$ and $^{\triangle\triangle\triangle}P < 0.001$ *vs* control group; $^{***}P < 0.001$ *vs* model group. IL-4: interleukin-4; IFN-γ: interferon-γ; LD-JBOL: low-dose JBOL group; MD-JBOL: medium-dose JBOL group; HD-JBOL: high-dose JBOL group.

pathic pulmonary fibrosis. TGF-β1 is one of the key cytokines involved in the pathogenesis of pulmonary fibrosis, which has been indicated to promote differentiation of fibroblasts into activated myofibroblasts, enhance collagen synthesis, and reduce collagen degradation, thus promoting the collagen deposition inside lung tissues (Leask & Abraham, 2004; Lee et al., 2004). The TGF-β1 concentration in the lung tissues of JBOL groups was significantly decreased compared with the model group, suggesting that JBOL may inhibit the expression of TGF-β1 and subsequently reduce the transformation of fibroblasts to myofibroblasts, as well as the collagen deposition. The combination of various methods may ensure the objectivity and accuracy of experimental results.

Following the BLM administration, increased numbers of inflammatory cells were observed and the secretion of TNF-α in rat lung tissue samples was enhanced. The concentration of TNF-α induced by BLM was significantly decreased by JBOL treatment. These results were consistent with previous studies and indicated that JBOL could significantly attenuate BLM-induced inflammation (Zhang et al., 2018).

The results also indicated that application of different doses of JBOL significantly diminished inflammation respected to the BLM administration. It was also observed that JBOL prevents the level of IL-4, which was an important proinflammatory cytokine and was mainly secreted from macrophages and a key cytokine of Th2. IL-4 has been also reported to induce collagen synthesis in fibroblasts and plays a major role in regulating inflammation and cell mediated immune responses (Aoudjehane et al., 2008; Van Dyken & Locksley, 2013). All of these processes have been implicated in the pathogenesis of pulmonary fibrosis, and increased IL-4 is noted in radiation-induced lung injury and fibrosis (Amini et al., 2018). These results have been extended to include the murine lung in the bleomycin-induced mouse model of pulmonary fibrosis, demonstrating that there is upregulation of IL-4 mRNA in mononuclear cells and macrophages at sites of active fibrosis (Gharaee-Kermani et al., 2003). Further *in vivo* evidence for the encouraging fibrosis role of IL-4 comes from the transgenic (knock-in) mice is associated with increased susceptibility to bleomycin-induced inflammation and pulmonary fibrosis (Huaux et al., 2003). In human studies, the progression of idiopathic pulmonary fibrosis is also associated with a sustained IL-4 production (Bao et al., 2014; Vasakova et al., 2007). These results of IL-4 upregulation support the present findings and provide a role for IL-4 in the pathogenesis of human IPF.

In contrast, the Th1 cytokine IFN-γ is known to suppress fibroblast proliferation and collagen synthesis in human and animal studies (Meinel, Pongratz, Rauch, & Straub, 2013; Vu, Chen, Foda, Smaldone, & Hasaneen, 2019). A previous study demonstrated that a higher proportion of the fibrosing alveolitis patients with impaired IFN-γ production have subsequently shown spontaneous lung functional deterioration (Pejman et al., 2014). In addition, the administration of IFN-γ *in vivo* can cause a reduction of extracellular matrix in animal models of fibrosis (Li et al., 2018). In this study, the Th1 response is limited by reduced IFN-γ after BLM administration, and the enhancement of the Th2 response is marked by increasing IL-4 levels. The ratio of IFN-γ/IL-4 in the BLM model group was significantly decreased compared to the control group. Our results showed that JBOL could increase the level of IFN-γ and reverse the ratio of IFN-γ/IL-4 when compared to the model group. Therefore, it was assumed that JBOL may possess the ability to improve bleomycin-induced inflammation and pulmonary fibrosis via inhibiting oxidative stress, inflammation and switching the Th1/Th2 shift in rats. However, whether these findings are reliable in IPF patients were not confirmed. Therefore, clinical study will be applied and further exploration will be carried out to confirm this point.

5. Conclusion

In conclusion, the present study demonstrates that JBOL may attenuate BLM-induced inflammatory cell infiltration, pro-inflammatory cytokine release and excessive collagen deposition in rats. The mechanism might be the reversion of Th1/Th2 shift caused by BLM. The present findings therefore suggest a potential protective effect of JBOL against idiopathic pulmonary fibrosis. Additional study is needed to clarify the underlying mechanism of action.

Declaration of Competing Interest

The authors declare that they have no known competing financial interests or personal relationships that could have appeared to influence the work reported in this paper.

Acknowledgements

The authors would like to thank Shandong Hongjitang Pharmaceutical Group Co., Ltd. for supplying us the Jinbei Oral Liquid.

The National Science and Technology Major Project for 'Significant New Drugs Development' (2018ZX09721004-010) provides financial support during the literature searching and experimental

materials, the Major Program of the National Natural Science Foundation of China (No. 81891012) provides financial support during the data analysis, the CAMS Innovation Fund for Medical Sciences (CIFMS) (No. 2017-I2M-1-013) provide financial support during the language revising and publication.

References

Amini, P., Saffar, H., Nourani, M. R., Motevaseli, E., Najafi, M., Ali Taheri, R., & Qazvini, A. (2018). Curcumin mitigates radiation-induced lung pneumonitis and fibrosis in rats. *International Journal of Molecular and Cellular Medicine, 7*(4), 212–219.

Aoudjehane, L., Pissaia, A. J., Scatton, O., Podevin, P., Massault, P. P., Chouzenoux, S., ... Conti, F. (2008). Interleukin-4 induces the activation and collagen production of cultured human intrahepatic fibroblasts via the STAT-6 pathway. *Laboratory Investigation, 88*(9), 973–985.

Bao, Z., Zhang, Q., Wan, H., He, P., Zhou, X., & Zhou, M. (2014). Expression of suppressor of cytokine signaling 1 in the peripheral blood of patients with idiopathic pulmonary fibrosis. *Chinese Medical Journal, 127*(11), 2117–2120.

El-Chemaly, S., Cheung, F., Kotliarov, Y., O'Brien, K. J., Gahl, W. A., Chen, J., ... Gochuico, B. R. (2018). The immunome in two inherited forms of pulmonary fibrosis. *Frontiers in Immunology, 9*, 76.

Euler, T., Valesky, E. M., Meissner, M., Hrgovic, I., Kaufmann, R., Kippenberger, S., & Zöller, N. N. (2019). Normal and keloid fibroblasts are differentially influenced by IFN-γ and triamcinolone as well as by their combination. *Wound Repair and Regeneration, 27*(5), 450–461.

Fernandez, I. E., & Eickelberg, O. (2012). New cellular and molecular mechanisms of lung injury and fibrosis in idiopathic pulmonary fibrosis. *Lancet, 380*(9842), 680–688.

Gharaee-Kermani, M., Nozaki, Y., Hatano, K., & Phan, S. H. (2003). Lung interleukin-4 gene expression in a murine model of bleomycin-induced pulmonary fibrosis. *Cytokine, 15*(3), 138–147.

Huang, X., He, Y., Chen, Y., Wu, P., Gui, D., Cai, H., ... Wang, L. (2016). Baicalin attenuates bleomycin-induced pulmonary fibrosis via adenosine A2a receptor related TGF-β1-induced ERK1/2 signaling pathway. *BMC Pulmonary Medicine, 16*(1), 132.

Huaux, F., Liu, T., McGarry, B., Ullenbruch, M., & Phan, S. H. (2003). Dual roles of IL-4 in lung injury and fibrosis. *Journal of Immunology, 170*(4), 2083–2092.

Leask, A., & Abraham, D. J. (2004). TGF-beta signaling and the fibrotic response. *FASEB Journal, 18*, 816–827.

Lee, C. G., Cho, S. J., Kang, M. J., Chapoval, S. P., Lee, P. J., Noble, P. W., ... Elias, J. A. (2004). Early growth response gene 1-mediated apoptosis is essential for transforming growth factor beta1-induced pulmonary fibrosis. *Journal of Experimental Medicine, 200*(3), 377–389.

Li, L. F., Kao, K. C., Liu, Y. Y., Lin, C. W., Chen, N. H., Lee, C. S., ... Yang, C. T. (2017). Nintedanib reduces ventilation-augmented bleomycin-induced epithelial-mesenchymal transition and lung fibrosis through suppression of the Src pathway. *Journal of Cellular and Molecular Medicine, 21*(11), 2937–2949.

Li, W., Liang, R., Huang, H., Wu, B., & Zhong, Y. (2018). Effects of IFN-γ on cell growth and the expression of ADAM33 gene in human embryonic lung Mrc-5 fibroblasts *in vitro*. *Journal of Asthma, 55*(1), 15–25.

Liu, Q. M., Chu, H. Y., Ma, Y. Y., Wu, T., Qian, F., Ren, X., ... Wang, J. C. (2016). Salvianolic acid B attenuates experimental pulmonary fibrosis through inhibition of the TGF-β signaling pathway. *Scientific Reports, 6*, 27610.

Luzina, I. G., Todd, N. W., Iacono, A. T., & Atamas, S. P. (2008). Roles of T lymphocytes in pulmonary fibrosis. *Journal of Leukocyte Biology, 83*(2), 237–244.

Meinel, T., Pongratz, G., Rauch, L., & Straub, R. H. (2013). Neuronal α1/2-adrenergic stimulation of IFN-γ, IL-6, and CXCL-1 in murine spleen in late experimental arthritis. *Brain, Behavior, and Immunity, 33*, 80–89.

Mojiri-Forushani, H., Hemmati, A. A., Khodadadi, A., & Rashno, M. (2018). Valsartan attenuates bleomycin-induced pulmonary fibrosis by inhibition of NF-κB expression and regulation of Th1/Th2 cytokines. *Immunopharmacology and Immunotoxicology, 40*, 225–231.

Pejman, L., Omrani, H., Mirzamohammadi, Z., Shahbazfar, A. A., Khalili, M., & Keyhanmanesh, R. (2014). The effect of adenosine A2A and A2B antagonists on tracheal responsiveness, serum levels of cytokines and lung inflammation in guinea pig model of asthma. *Advanced Pharmaceutical Bulletin, 4*(2), 131–138.

Peng, R., Sridhar, S., Tyagi, G., Phillips, J. E., Garrido, R., Harris, P., ... Stevenson, C. S. (2013). Bleomycin induces molecular changes directly relevant to idiopathic pulmonary fibrosis: A model for "active" disease. *PLoS ONE, 8*(4) e59348.

Strongman, H., Kausar, I., & Maher, T. M. (2018). Incidence, prevalence, and survival of patients with idiopathic pulmonary fibrosis in the UK. *Advances in Therapy, 35*(5), 724–736.

Sumida, A., Hasegawa, Y., Okamoto, M., Hashimoto, N., Imaizumi, K., Yatsuya, H., ... Kawabe, T. (2008). TH1/TH2 immune response in lung fibroblasts in interstitial lung disease. *Archives of Medical Research, 39*(5), 503–510.

Tang, J., Lei, L., Pan, J., Zhao, C., & Wen, J. (2018). Higher levels of serum interleukin-35 are associated with the severity of pulmonary fibrosis and Th2 responses in patients with systemic sclerosis. *Rheumatology International, 38*(8), 1511–1519.

Van Dyken, S. J., & Locksley, R. M. (2013). Interleukin-4- and interleukin-13-mediated alternatively activated macrophages: Roles in homeostasis and disease. *Annual Review of Immunology, 31*, 317–343.

Vasakova, M., Striz, I., Slavcev, A., Jandova, S., Dutka, J., Terl, M., ... Sulc, J. (2007). Correlation of IL-1alpha and IL-4 gene polymorphisms and clinical parameters in idiopathic pulmonary fibrosis. *Scandinavian Journal of Immunology, 65*(3), 265–270.

Vu, T. N., Chen, X., Foda, H. D., Smaldone, G. C., & Hasaneen, N. A. (2019). Interferon-γ enhances the antifibrotic effects of pirfenidone by attenuating IPF lung fibroblast activation and differentiation. *Respiratory Research, 20*(1), 206.

Wang, Y. C., Dong, J., Nie, J., Zhu, J. X., Wang, H., Chen, Q., ... Shuai, W. (2017). Amelioration of bleomycin-induced pulmonary fibrosis by chlorogenic acid through endoplasmic reticulum stress inhibition. *Apoptosis, 22*(9), 1147–1156.

Wynn, T. A. (2004). Fibrotic disease and the T (H)1/T(H)2 paradigm Nature reviews. *Immunology, 4*(8), 583–594.

Yasui, H., Gabazza, E. C., Tamaki, S., Kobayashi, T., Hataji, O., Yuda, H., ... Taguchi, O. (2001). Intratracheal administration of activated protein C inhibits bleomycin-induced lung fibrosis in the mouse. *American Journal of Respiratory and Critical Care Medicine, 163*(7), 1660–1668.

Yoshimoto, T. (2018). The hunt for the source of primary interleukin-4: How we discovered that natural killer T cells and basophils determine T helper type 2 cell differentiation *in vivo*. *Frontiers in Immunology, 9*, 716.

Zhang, C. H., Cui, Q. H., Tian, J. Z., Wang, P., Hou, L., Gong, T., ... Zhu, Q. J. (2018). Effect of Jinbei oral liquid on bleomycin-induced pulmonary fibrosis in rats. *Pharmacology and Clinics of Chinese Materia Medica, 34*, 146–150.